Supporting Information

Two-dimensional calcium terephthalate as low-cost, high-performance anode for sodium-ion batteries

Dandan He,[a] Yang Liu,*[a,b] Yangyang Fan,[a] Changwei Dun,[a] Yun Qiao*[b] and Shulei Chou*[c]

[a] *School of Chemistry and Chemical Engineering, Key Laboratory of Green Chemical Media and Reactions, Ministry of Education, Henan Normal University, Xinxiang, Henan 453007, China. E-mail: liuy986@htu.edu.cn.*

[b] *School of Environment and Chemical Engineering, Shanghai University, Shanghai, 200444, China. E-mail: yunqiao@shu.edu.cn.; liuy986@shu.edu.cn.*

[c] *Institute for Carbon Neutralization, College of Chemistry and Materials Engineering, Wenzhou University, Zhejiang, 325035, China. E-mail: chou@wzu.edu.cn.*

Experimental section

Synthesis of CaTP with different morphologies

Typically, 4.15 g terephthalic acid was added into 0.33 mol/L, 150 mL sodium hydroxide solution. The mixture was stirred at the room temperature to make sure the complete dissolution of terephthalic acid. And then, the aqueous mixed solution was evaporated at 80 °C in an electric oven to obtain the Na_2TP crystals (Figure S1).

The preparation of CaTP: 0.21 g Na_2TP was added into 20 mL 4.5 mM hexadecyl trimethyl ammonium bromide (CTAB) solution with ethanol and de-ionized water (DI) as solvents under vigorous stirring. Afterwards, 0.11 g anhydrous $CaCl_2$ was dissolved in 10 mL ethanol and DI, and then this solution was added into the above transparent solution drop by drop under stirring. Subsequently, the mixed solution was transferred into a stainless autoclave and heated up to 110 °C for 1 hour in an electric oven. The resulting precipitates were centrifuged, washed with DI and ethanol, and finally dried at 80 °C in vacuum overnight. The volume ratios of DI water and ethanol is 4:1, 2:1 and 1:1, the corresponding samples were marked as CaTP-BL, CaTP-SL and CaTP-SH, respectively. As a comparison, ethanol was replaced by glycerol or polyethylene glycol to synthesize CaTP with the same conditions for the volume ratios of DI water and glycerol or polyethylene glycol to 1:1. In addition, the CaTP was prepared without using ethanol and the other conditions are the same. Moreover, the CTAB as surfactant were added to prepare CaTP, in which the concentration of CTAB are 0 mM, 3.6 mM and 5.4 mM, respectively.

Characterization

The fourier transform infrared (FTIR) spectra were employed to analyze the crystal structure, which were diluted with KBr. The X-ray diffraction (XRD; D8 Advance Bruker) patterns were recorded using Cu-Kα radiation from 2θ=5–80°. The morphologies of samples were characterized by the field-emission scanning electron microscope (FESEM; JSM-6700F) and high-resolution transmission electron microscope (HRTEM; JEOL JEM-2100).

Electrochemical measurements

The electrochemical performances were tested by the coin-type cells (size:2032) assembled in an argon-filled glove-box (H_2O, O_2 < 0.1 ppm). 60 wt% active materials, 30 wt% Super-P and 10 wt% sodium alginate were mixed by deionized water, which were then coated on Cu foil and dried in vacuum at 80 °C to prepare the working electrode. The Na metallic foil and glass fiber were used as the counter electrode and separator, respectively. The electrolyte was 1 M $NaClO_4$ in ethylene carbonate (EC) and propylene carbonate (PC) (V:V=1:1) with 5 vol% nonreactive fluoroethylene carbonate (FEC) additives. Cyclic voltammetry (CV) was evaluated on the electrochemical workstation (CHI760E). Galvanostatic charge and discharge was performed on Land testing system (CT2001A) with the voltage range of 0-3 V.

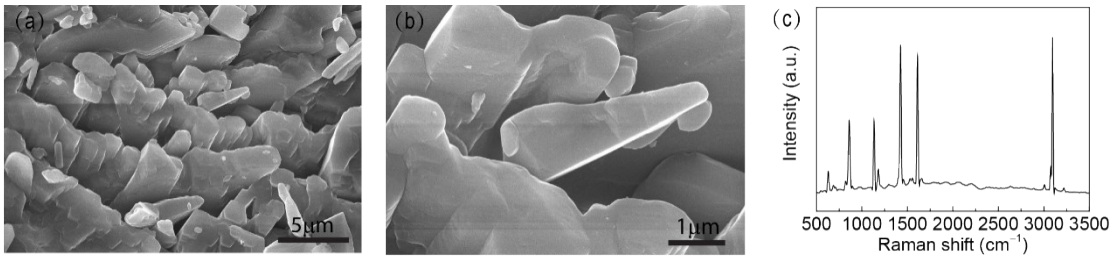

Figure S1. (a, b) FESEM images and (c) Raman spectrum of Na_2TP.

The morphologies of Na_2TP are shown in Figure S1a and S1b, which is composed of irregular layer particles. The Raman spectrum of Na_2TP is displayed in Figure S1c. The bonds at about 629 and 688 cm^{-1} are ascribed to the bending modes of COO^- group.[1] The CH out-of-plane deformations are range from 780 to 1000 cm^{-1}. And the bonds between 1000 and 1800 cm^{-1} are similar with the samples of CaTP. The CH stretching modes of the phenyl ring in Na_2TP are observed in the region 3120–3005 cm^{-1}. These results are in accordance with the previous work.[1]

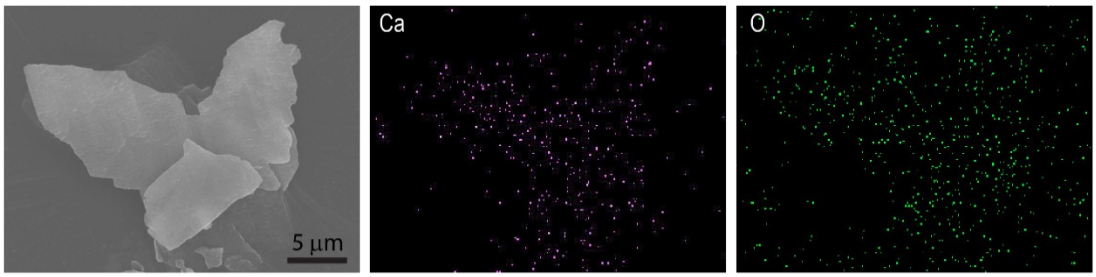

Figure S2. EDX elemental mapping images of the sample.

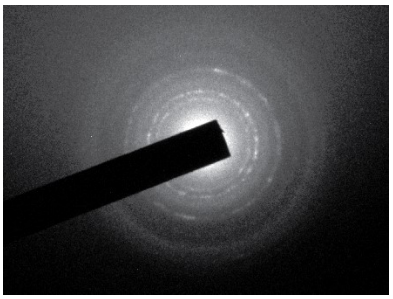

Figure S3. The electron diffraction pattern of CaTP.

The structure information of CaTP have been investigated by the previous work.[2, 3] The electron diffraction pattern were carried out from JEOL JEM-2100 electron microscope, which reveals polycrystallinity feature of CaTP.

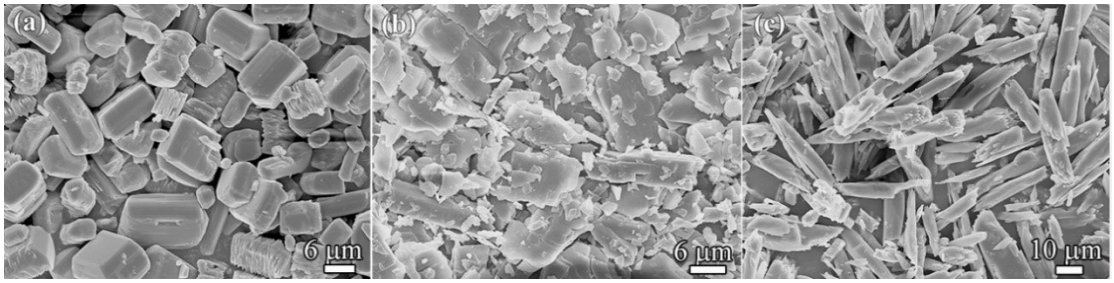

Figure S4. SEM images of the CaTP as the control samples: (a) without alcohol, (b) glycerol and (c) polyethylene glycol.

It is found that the organic solvent in the reactive solutions has great effects on the dimensions and morphologies of final products. The effect of ethanol is further investigated. Without ethanol, the sample is composed of abundant micro-blocks, which is similar to CaTP-BL, while the surface is relatively smooth (Figure S4a). This means that the ethanol possesses the significantly enhanced capping ability with the increase of its amount, thus the crystal growth is remarkably restricted to form 2D sheet. Meanwhile, ethanol was replaced by glycerol or polyethylene glycol and their ratios to DI water are 1:1 under the same reaction conditions. It can be seen that the sample obtained using glycerol is composed with irregular sheet and large block shape (Figure S4b). Moreover, the as-prepared sample using polyethylene glycol is consist of microrods with cracked ends (Figure S4c). These results indicate that the alcohols with different chain length have a great effect on the final morphology of CaTP.

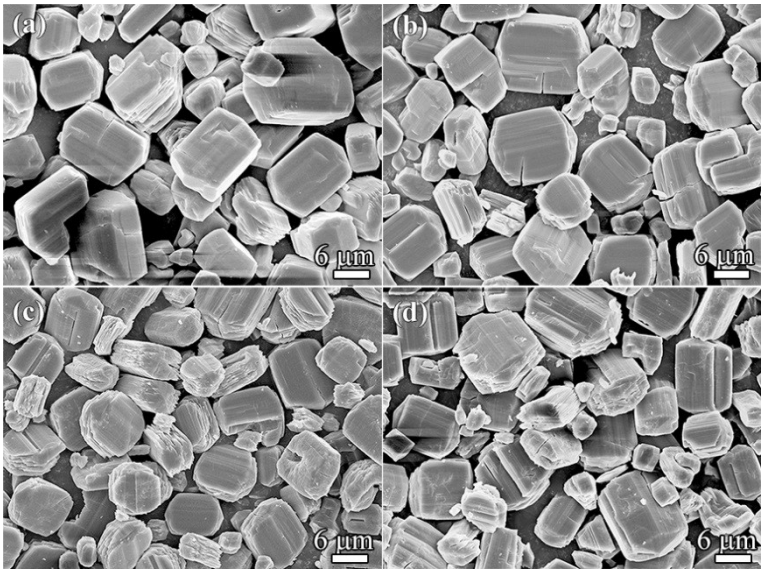

Figure S5. SEM images of CaTP were obtained by using (a) 0 mM, (b) 3.6 mM, (c) 4.5 mM and (d) 5.4 mM CTAB as surfactant.

The effect of surfactant on 2D sheet sample was investigated when the volume ratio of DI water and ethanol is 1:4. When the content of CTAB is increased from 0 to 5.4 mM, all the samples can maintain the block shapes, as shown in Figure S5. It is worth to mention, the CaTP with 4.5 mM CTAB displays more regular and uniform distribution, and much smaller size than the other three samples. This indicates that CTAB plays an important role morphology control of CaTP.

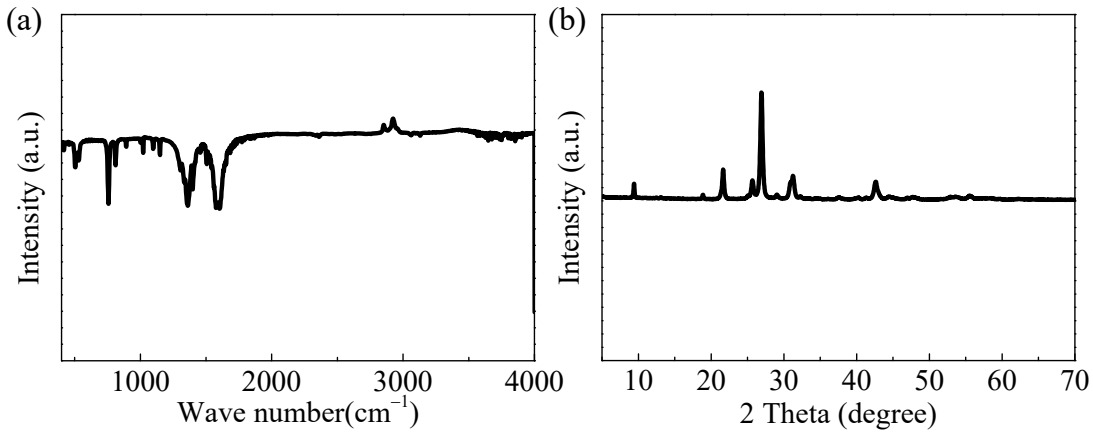

Figure S6. (a) FTIR spectrum and (b) XRD pattern of pure CaTP without any other additives.

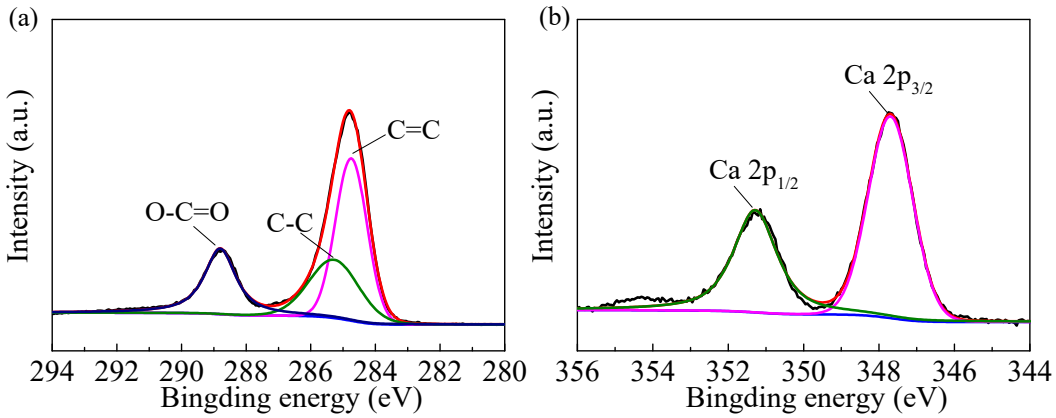

Figure S7. High resolution XPS spectra of (a) C1s and (b) Ca 2p for CaTP-BL.

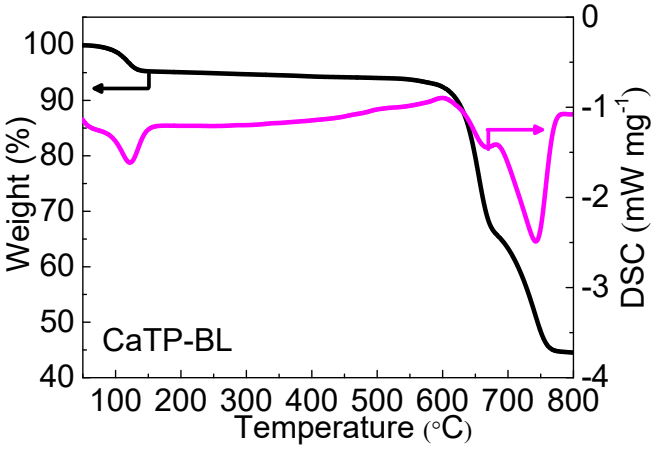

Figure S8. TGA and DSC curves of CaTP-BL.

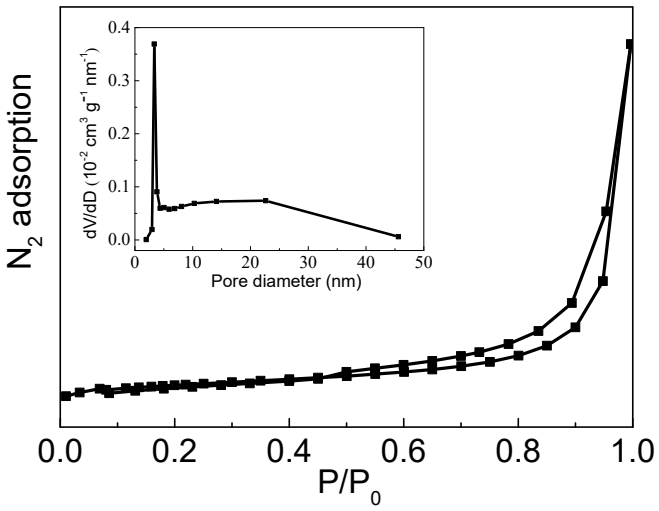

Figure S9. Nitrogen adsorption–desorption isotherms of CaTP- BL (inset: the pore size distribution curve).

As shown in Figure S9, the isotherms display a hysteresis loop at a relative-pressure range of 0.5 and 1, which can be classified as IV isotherms for CaTP-BL. The Barrett-Joyner-Halenda (BJH) pore size distribution displays the pores are about 27 nm. Moreover, the BET specific surface area and pore volume are only about 8.8 $m^2\ g^{-1}$ and 0.06 $cm^3\ g^{-1}$, respectively.

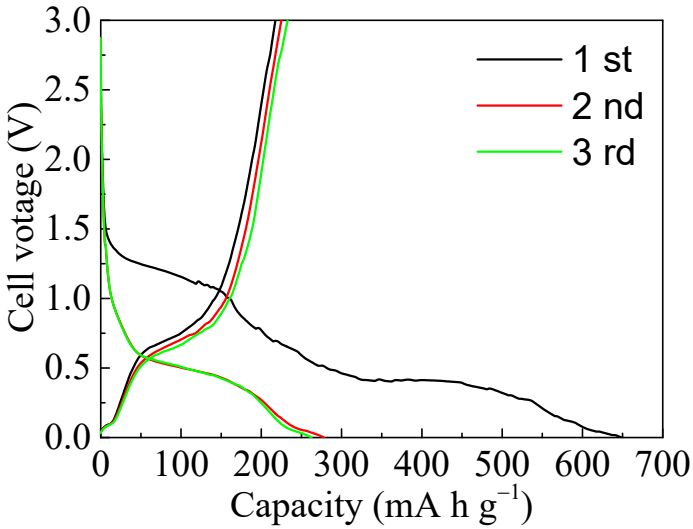

Figure S10. Disharge–charge curves at a current density of 25 mA g^{-1} for the CaTP-SH electrode with different amount of active materials.

Figure S10 displays the discharge and charge profiles of CaTP-SH with 70% active materials at a current density of 25 mA g^{-1} with the voltage between 0 and 3.0 V. It can be seen that the first discharge and charge capacities are 711.2 and 234.6 mA h g^{-1}, respectively. During the third cycle, the discharge and charge capacities are 288.5 and 248.6 mA h g^{-1}, respectively. The CaTP electrode consisted with Ca, C, H, O can be a low-cost electrode and deliver a high specific capacity with appropriate material design for sodium ion battery, thus will display a great potential application in the field of energy storage.

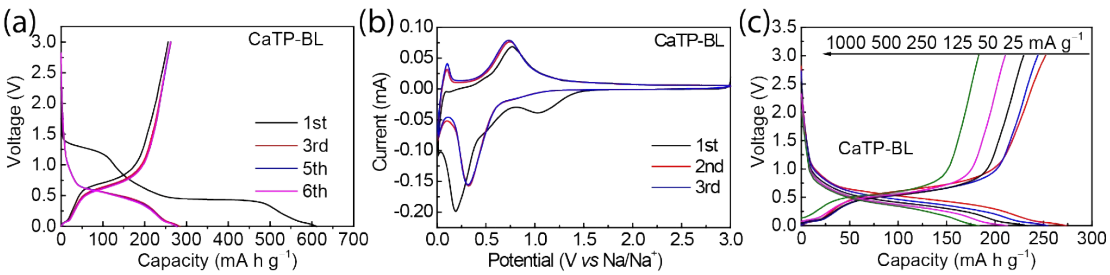

Figure S11. Electrochemical performance of the CaTP-BL: (a) Disharge–charge curves at a current density of 25 mA g^{-1}, (b) CV curves at a scan rate of 0.2 mV s^{-1} from 0 to 3.0 V, and (c) charge and discharge curves at various current densities.

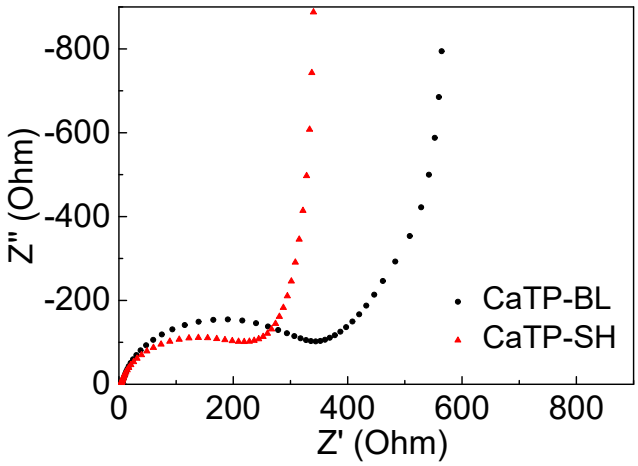

Figure S12. Electrochemical impedance spectra for CaTP-BL and CaTP-SH.

The Nyquist plots show that the diameter of the semicircle for CaTP-SH in the high–medium frequency region is much smaller than that of CaTP-BL, indicating that CaTP-SH has lower contact and charge-transfer impedance. For the low-frequency slope line, the slope angle for CaTP-SH is steeper than that of CaTP-BL, manifesting its fast Na^+ ions diffusivity. Therefore, CaTP-SH as electrode shows low contact and charge-transfer impedance.

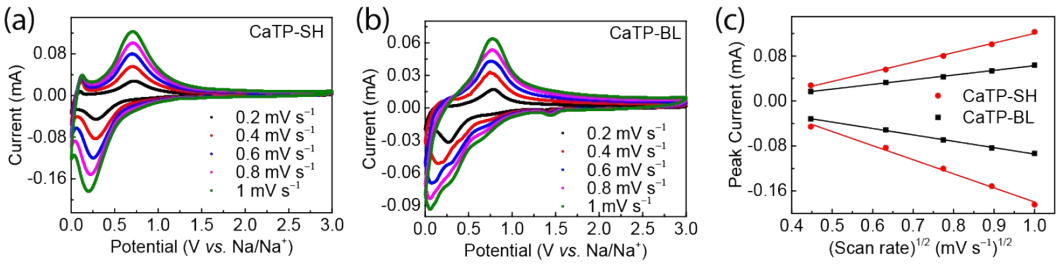

Figure S13. CV curves of the CaTP-SH (a) and CaTP-BL (b) samples at different scan rates. (c) linear fitting of the peak current versus (scan rate)$^{1/2}$.

The CV curves have been tested within a potential range from 0.0 to 3.0 V at various scan rates. The overall CV shape maintains well as the scan rate increased from 0.2 to 1.0 mV s^{-1}. The voltage gap between the reduction and oxidation peaks is attributed to the electrode polarization, closely correlating with the conductivity of the active material. The apparent diffusion coefficients of sodium ions for CaTP-BL and CaTP-SH electrode were calculated from the slop of peak current versus the square root of the scan rate ($v^{1/2}$), according to the Randles-Sevcik Equation:[4]:

$$I_p=0.4463n^{3/2}F^{3/2}CAR^{-1/2}T^{-1/2}D^{1/2}v^{1/2}$$

I_p is the peak current (A), n is the number of electrons, F is Faraday constant (96485 C mol^{-1}), C is the bulk concentration in moles per cubic centimeter (mol cm^{-3}), A is the area of the electrode (cm^2), R is the gas constant (8.314 J mol^{-1} K^{-1}), T is the absolute temperature (K), D is the sodium ions apparent diffusion coefficient (cm^2 s^{-1}), and v is the potential scan rate in volts per second (V s^{-1}).

As show in Figure S13, the CaTP-SH displays an apparent higher diffusion coefficient in contrast to CaTP-BL, indicating the higher kinetics of sodium ions extraction and insertion within CaTP-SH.[5]

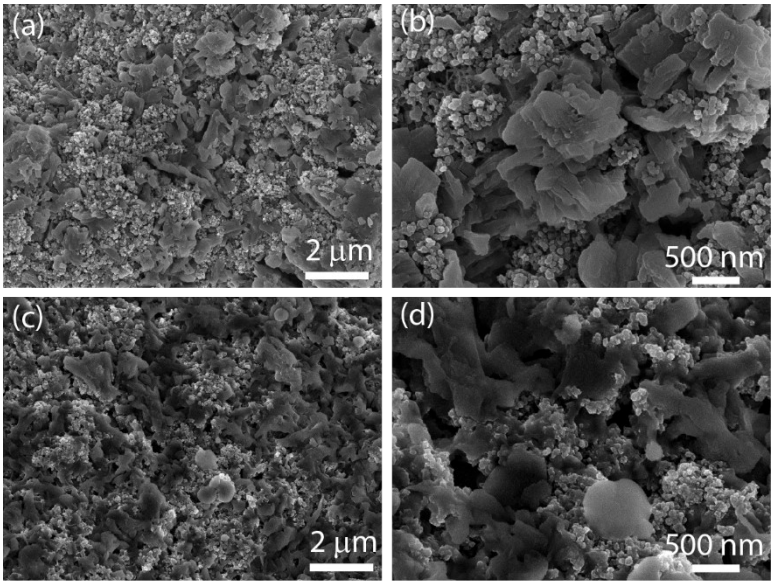

Figure S14. The SEM images of the CaTP anode, (a, b) pristine, (c, d) after discharge and charge process.

References

[1] H. T. Varghese, C. Y. Panicker, D. Philip, K. Sreevalsan and V. Anithakumary, *Spectrochimica Acta Part A: Molecular and Biomolecular Spectroscopy*, **2007**, *68*, 817-822.

[2] T. Matsuzaki and Y. Iitaka, *Acta Crystallogr., Sect. B: Struct. Sci., Cryst. Eng. Mater.*, **1972**, *28*, 1977-1981.

[3] Y. Li, H. Yi, M. Ge and D. Yao, *Macromol. Mater. Eng.*, **2021**, *306*, 2100591.

[4] Q. Wei, X. Chang, J. Wang, T. Huang, X. Huang, J. Yu, H. Zheng, J. Chen and D. Peng, *Adv. Mater.*, **2022**, *34*, 2108304.

[5] Z. Liu, B. Liu, P. Guo, X. Shang, M. Lv, D. Liu and D. He, *Electrochim. Acta*, **2018**, *269*, 180-187.